

## **Hopping magnetoresistance in strongly disordered monolayer graphene**

E. Zion<sup>1</sup>, A.V. Butenko<sup>1</sup>, I. Shlimak<sup>2†</sup>, L. Wolfson<sup>2</sup>, V. Richter<sup>1</sup>, Yu. Kaganovskii<sup>2</sup>,  
A. Sharoni<sup>1</sup>, A. Haran<sup>3‡</sup>, D. Naveh<sup>3</sup>, E. Kogan<sup>2</sup>, M. Kaveh<sup>2</sup>

<sup>1</sup>*Department of Physics and Institute of Nanotechnology and Advanced Materials, Bar-Ilan University, Ramat-Gan 52900, Israel*

<sup>2</sup>*Jack and Pearl Resnick Institute of Advanced Technology, Department of Physics, Bar-Ilan University, Ramat-Gan 52900, Israel*

<sup>3</sup>*Faculty of Engineering, Bar-Ilan University, Ramat-Gan 52900, Israel*

### Abstract

Magnetoresistance (MR) of ion irradiated monolayer graphene samples with variable-range hopping (VRH) mechanism of conductivity was measured at temperatures down to  $T = 1.8$  K in perpendicular and parallel magnetic fields up to  $B = 8$  T. It is shown that in perpendicular magnetic fields, conductivity increases, or negative MR (NMR) is observed, while parallel magnetic field results in positive MR (PMR) at low temperatures. NMR is explained on the basis of the “orbital” model in which magnetic field suppresses the destructive interference of many paths through the intermediate sites in the total probability of the long-distance tunneling in the VRH regime. Samples with different degree of disorder were studied systematically. It is found that all NMR curves for different samples and different temperatures are merged into one common curve when plotted as a function of  $B/B^*$ , where  $B^*$  is experimentally determined magnetic field at which the quadratic dependence of NMR on  $B$  is replaced by the linear one. It is shown that  $B^* \sim T^{1/2}$  in agreement with theoretical predictions. The obtained values of  $B^*$  allowed to determine the localization radius  $\xi$  for different samples. It is shown that  $\xi$  decreases expectedly with increase of disorder. PMR in parallel magnetic fields is explained by the alignment of electron spins which results in suppression of hopping transitions via double occupied states.

### Introduction

Defects are very useful tool to modify and control the physical properties of true two-dimensional (2d) material – monolayer graphene and, therefore, disordered graphene attracts a lot of attention [1-7]. The evolution of optical (Raman spectra) and electronic (conductivity) properties of graphene with increasing disorder has been investigated in many papers (see, for example, [8-11]). It has been shown that increase of disorder leads to change of the conductivity mechanism from metallic one in pristine films to the conductivity determined by the regime of weak localization-antilocalization, and then conductivity is realized by means of variable-range hopping (VRH) of localized charge carriers in strongly disordered samples.

In this work, we report the results of magnetoresistance (MR) measurements in monolayer graphene samples strongly disordered with ion irradiation. MR in the VRH regime of conductivity has been observed earlier in different graphene-based structures: fluorinated graphene [4], graphene exposed to ozone [5], graphene oxide [6]. In Ref. [7],

MR was measured in monolayer graphene flakes subjected to  $\text{Ga}^+$  ion irradiation. In one highly disordered sample, the negative MR was observed which was attributed to the crystalline-boundary scattering. In Ref. [9], disorder in graphene was introduced by  $\text{C}^+$  ion irradiation with energy 35 keV. It was shown that at high dose of irradiation, the conductivity is described by the VRH mechanism, but no MR measurements were conducted. We are not aware about measurements of hopping MR in series of monolayer graphene samples with different degree of disorder and attempts of merging these dependences.

### Experimental results and discussion

The investigated samples belong to a series of samples gradually disordered by different dose of ion irradiation. All samples were fabricated by means of electron-beam lithography (EBL) on the common large-scale (5x5 mm) monolayer graphene film and divided into 6 groups. Initial sample before EBL was marked as sample 0. The samples from the first group, marked as sample 1, were not irradiated, while 5 others groups were subjected to different doses (from  $5 \times 10^{13}$  up to  $1 \times 10^{15} \text{ cm}^{-2}$ ) of irradiation with carbon ions with energy 35 keV. In Ref. [10], concentration of structural defects  $N_D$  was determined for each group using measurements of the Raman scattering. For samples 1–4, the values of  $N_D$  in units of  $10^{12} \text{ cm}^{-2}$  are 1, 3, 6 and 12 correspondingly. In Ref. [11], it was shown that the temperature dependence of resistivity  $R(T)$  in initial sample 0 has a metallic character, while in slightly irradiated sample 1, conductivity is characterized by the regime of "weak localization-antilocalization" (WL-WAL). Measurements of MR in this sample showed a remarkable agreement with theoretical model [12]. In more irradiated samples 2, 3 and 4, dependences  $R(T)$  are described by the variable-range hopping (VRH) of strongly localized carriers. The strength of localization increases from sample 2 to sample 4. It was shown in [11], that in samples 3 and 4, both regimes of VRH were observed with decreasing  $T$ .

As known, the form of  $R(T)$  in VRH depends on the structure of the density-of-states  $g(\varepsilon)$  in the vicinity of the Fermi level (FL)  $\mu$  [13]: when  $g(\mu) \neq 0$  and is nearly constant,  $R(T)$  is described by the "Mott VRH" which in 2d has the form of " $T^{-1/3}$ -law":

$$R(T) = R_0 \exp(T_M/T)^{1/3}, \quad T_M = C_M [g(\mu) \zeta^2]^{-1} \quad (1)$$

Here  $R_0$  is a prefactor,  $C_M = 13.8$  is the numerical coefficient,  $\zeta$  is the radius of localization.

The Coulomb interaction between localized carriers leads to their redistribution in the vicinity of the FL. This results in a soft Coulomb gap around FL, which in 2d has a linear form  $g(\varepsilon) = |\varepsilon - \mu|(\kappa/e^2)$  with  $g(\mu) = 0$ . In this case, VRH is described by the "Efros-Shklovskii (ES) VRH" or " $T^{-1/2}$ -law":

$$R(T) = R_0 \exp(T_{ES}/T)^{1/2}, \quad T_{ES} = C_{ES} (e^2/\kappa \zeta) \quad (2)$$

Here  $C_{ES} = 2.8$  is the numerical coefficient,  $\kappa$  is the dielectric constant of the material.

MR of samples 2, 3 and 4 was measured at temperatures down to 1.8 K in magnetic fields up to  $B = 8\text{T}$  in perpendicular  $B_{\perp}$  and in-plane (parallel)  $B_{\parallel}$  geometry. It was observed that  $B_{\perp}$  leads to the increase of conductivity, or negative MR (NMR) in contrast with  $B_{\parallel}$  which results in positive MR (PMR) at low temperatures, Fig. 1. This strong anisotropy shows unambiguously that NMR in perpendicular fields is determined by the orbital mechanisms, while PMR in parallel fields is determined by the spin polarization. In that order we will discuss the results of measurements.

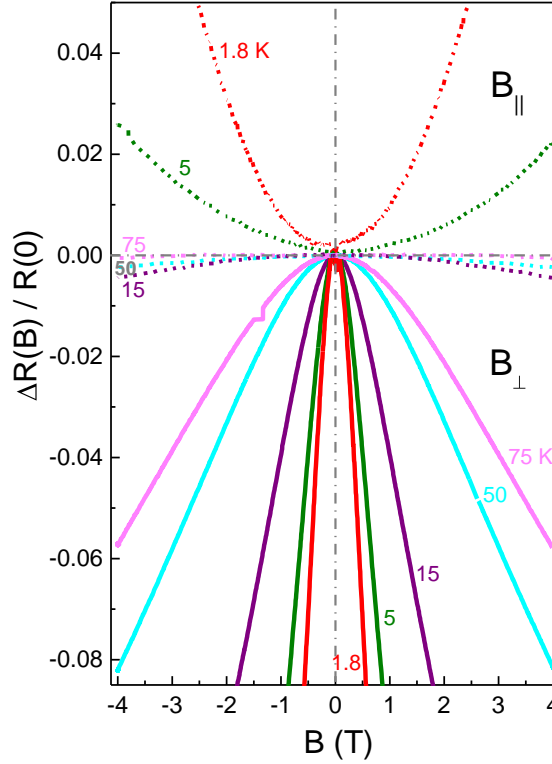


Fig. 1.  $\Delta R/R$  as a function of  $B$  for sample 3 in parallel and perpendicular magnetic fields at different temperatures shown near each curve.

### Negative MR in perpendicular magnetic fields

Fig. 2 shows the MR curves  $\Delta R(B)/R(0) \equiv [R(B) - R(0)]/R(0)$  at different  $T$  for all three samples on a linear scale. One can see the square dependence at very low fields (more pronounced for sample 4) followed by a "quasilinear" and then "sublinear" dependences. One can see also, that NMR at fixed  $T$  decreases with increase of disorder from sample 2 to 4. For sample 4, NMR first increases with decreasing  $T$ , while at  $T < 10\text{ K}$ , NMR rapidly decreases and the curves seek to change the sign. It could be due to the standard positive MR caused by the shrinkage of the wave functions in the perpendicular magnetic fields [13]. Therefore we will discuss the NMR for sample 4 only down to 10 K.

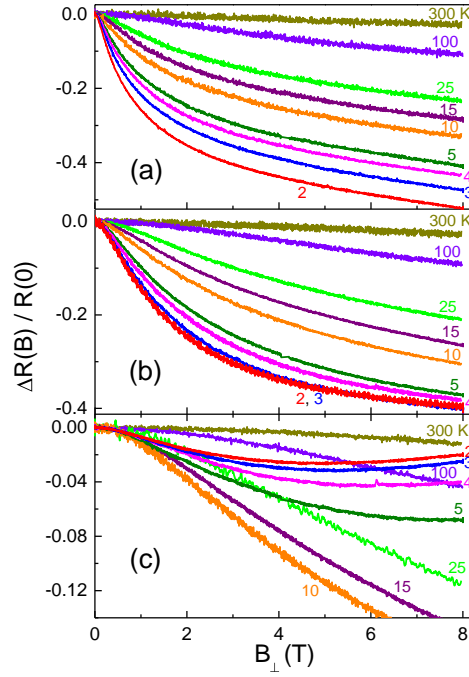


Fig. 2. NMR of samples 2 (a), 3 (b) and 4(c) at different temperatures ( $T$ , K) shown near the curves. The density of structural defects  $N_D$  ( $\text{cm}^{-2}$ ): in sample 2 –  $3 \times 10^{12}$ , 3 –  $6 \times 10^{12}$ , 4 –  $1.2 \times 10^{13}$ .

Fig. 3 shows the NMR data for all samples plotted on the log-log scale. On this scale, the slope to the curve is equal to the power  $\alpha$  in  $\Delta R/R \sim B^\alpha$ . Quadratic dependence ( $\alpha = 2$ ) is observed at low fields up to some value  $B^*$ .

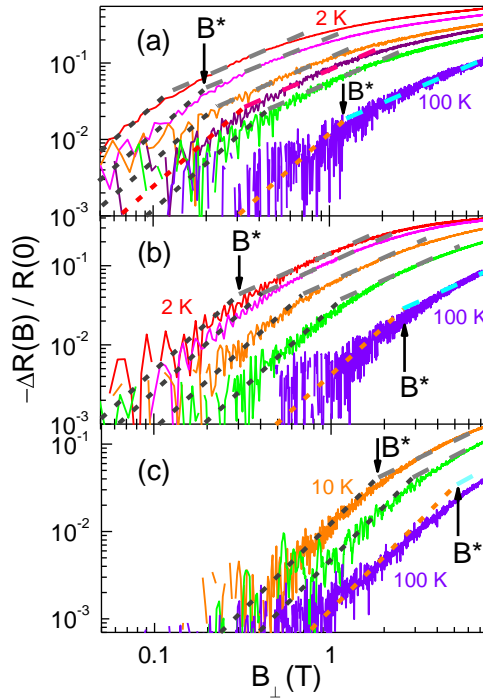


Fig. 3. NMR as a function of  $B$  plotted on the log-log scale for samples 2 (a), 3 (b) and 4 (c). Short dashed lines correspond to  $\alpha = 2$ , dashed lines to  $\alpha = 1$ .  $B^*$  shows the end of quadratic dependence.

Very weak effect of NMR (about 1-2%) was earlier observed in three-dimensional (3d) Mott VRH in heavily doped and compensated Ge and explained by the shift in the position of the Fermi level  $\mu$  in the density-of-states  $g(\varepsilon)$  induced by spin polarization which results in small change of  $g(\mu)$  and corresponding change of parameter  $T_M$ , Eq. (1), which in turn determines the sample resistance in Mott VRH (for a review, see [14]).

In 2d systems, a significant NMR in the VRH regime has been observed in perpendicular magnetic fields [15-20]. Anisotropy of this effect in perpendicular and parallel fields unambiguously indicates the orbital nature of NMR, because effects due to spin polarization has to be isotropic. Theoretically the effect of orbital NMR in the VRH regime of conductivity has been discussed in [21-26]. The main idea of explanation suggested by Nguen, Spivak and Shklovskii [21] is based on the following consideration.

As known, in VRH, only part of localized states with energy levels in so-called "optimal band" around FL  $\varepsilon(T)$  are involved in the hopping process, the width of  $\varepsilon(T)$  decreases with temperature [13]:

$$\varepsilon(T) = T^{2/3} [g(\mu) \xi^2]^{-1/3} \quad (3)$$

Correspondingly the hopping distance  $r_h$  increases, which gives  $r_h \sim T^{1/3}$ :

$$r_h \approx [g(\mu) \varepsilon(T)]^{-1/2} \approx \xi (T_M/T)^{1/3} \quad (4)$$

Therefore, at low  $T$ ,  $r_h$  becomes much larger than the mean distance between localized centers, and the probability of the long-distance hop is determined by the interference of many paths of the tunneling through the intermediate sites which include scattering process (Fig. 4). All these scattered waves together with non-scattered direct wave contribute additively to the amplitude of the wave function  $\Psi_{12}$  which reflects the probability for a charge carrier localized on site 1 to appear on site 2. An important feature is that there is no backscattering, and scattered waves decay rapidly with increasing distance as  $\exp(-2r/\xi)$ , therefore only the shortest paths contribute to  $\Psi_{12}$ . All these paths are concentrated in a cigar-shaped domain of the length  $r_h$ , width  $D \approx (r_h \xi)^{1/2}$  and area  $A \approx r_h^{3/2} \xi^{1/2}$ .

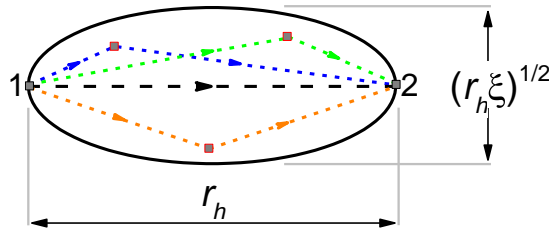


Fig. 4. Schematics of the cigar-shaped region with localized states contributing to the probability of an electron tunneling from center 1 to center 2.

As a result of averaging over different configurations, the contribution of the scattered sites to the total hopping probability vanishes due to destructive interference. The perpendicular magnetic field suppresses the interference which leads to the increase of the hopping probability and, therefore, to the negative MR. Taking into account that the hopping distance  $r_h$  is fixed, the increase of the hopping probability could be considered as

a small increase of the localization radius  $\xi$ . Both VRH parameters  $T_M$  and  $T_{ES}$  depend on the value of  $\xi$ , but differently:  $T_M \sim \xi^2$ , Eq. (1), while  $T_{ES} \sim \xi^1$ , Eq. (2). This gives rise to a suggestion that NMR has to be stronger for the case of the Mott VRH, then that for the ES VRH. This prediction was observed in experiment. In Fig. 5(a), the temperature dependences of the modulus of NMR at fixed magnetic field  $B = 4$  T for samples 2, 3 and 4 are shown. One can see that NMR increases with decreasing  $T$  linearly with  $T^{-1/3}$  and deviates from the straight line to smaller values at approximately the same temperatures where  $R(T)$  deviates from the Mott VRH ( $T^{-1/3}$ -law) to the stronger ES VRH ( $T^{-1/2}$ -law), Fig. 5(b).

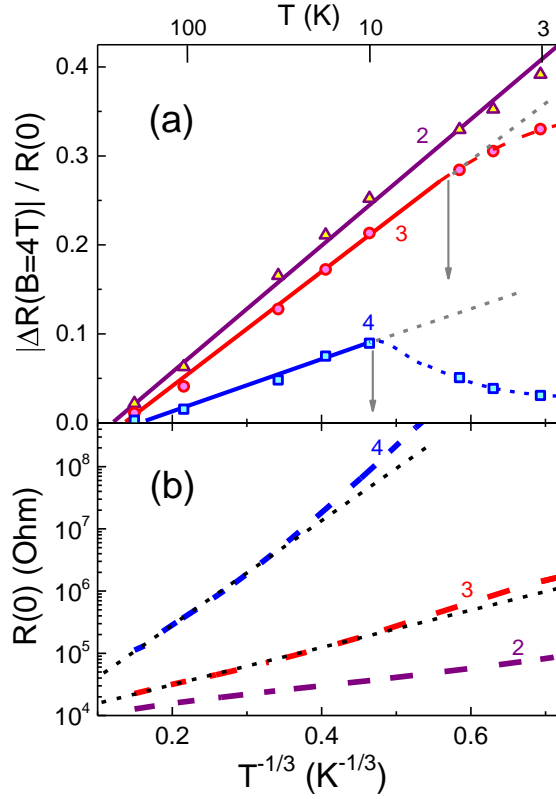


Fig. 5. (a)–modulus of NMR at fixed magnetic field  $B = 4$  T for samples 2, 3, 4 plotted as a function of  $T^{-1/3}$ . (b) - temperature dependence  $R(T)$  for these samples at zero magnetic field.

In accordance with theoretical considerations [21-26], NMR as a function  $B$  is linear at moderate fields and quadratic at very low fields. It is naturally to determine the magnetic field scale using the ratio  $\eta = \Phi_B / \Phi_0$  where  $\Phi_0 = h/2e \approx 2.07 \times 10^{-15}$  W is the magnetic flux quantum and  $\Phi_B = B \cdot A$  is the magnetic flux through the average cigar-shape area. At low fields ( $\eta \ll 1$ ), the  $B^2$ -dependence has to be observed, while at  $\eta > 1$ , it will be replaced by the linear one, so the condition  $\eta = 1$  determines the magnetic field  $B^*$  of the crossover:  $B^* = \Phi_0 / A \sim r_h^{-3/2} \xi^{-1/2}$ . Some values of  $B^*$  are shown in Fig. 3 by arrows. Taking into account Eq. (4), one get

$$B^* = \Phi_0 \xi^{-2} (T_M / T)^{-1/2} = \lambda T^{1/2}, \quad \lambda = \Phi_0 \xi^{-2} T_M^{-1/2} \quad (5)$$

In Fig. 6,  $B^*$  for all samples is plotted as a function of  $T^{1/2}$ . One can see that, indeed,  $B^* \sim T^{1/2}$ . Coefficient  $\lambda$  is equal to 0.1, 0.24 and 0.58 T K<sup>-1/2</sup> for samples 2, 3 and 4. Knowledge

of  $\lambda$  allows us to estimate the value of localization radius  $\xi$ . For samples 2, 3 and 4, with  $T_M = 68, 308$  and  $5960$  K [11], this gives  $\xi \approx 50, 22$  and  $7$  nm correspondingly, which looks quite reasonable:  $\xi$  decreases with increase of disorder (from sample 2 to sample 4).

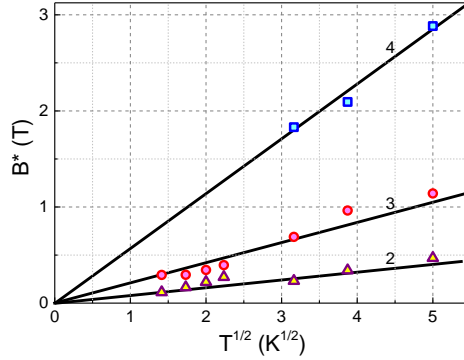


Fig. 6. The values of  $B^*$  as a function of  $T^{1/2}$ . The sample numbers are shown near the straight lines..

We also use the values of  $B^*$  in an attempt to merge the NMR data for all samples and all temperatures below 25 K. In Fig. 7, MR curves from Fig. 2 are plotted as a function of dimensionless parameter  $B/B^*$ . One can see that all curves are merged in one common dependence which completely describes the NMR in our samples. It is to be hoped that the analytical expression of this curve will be obtained in the future extended theory of orbital NMR in VRH regime.

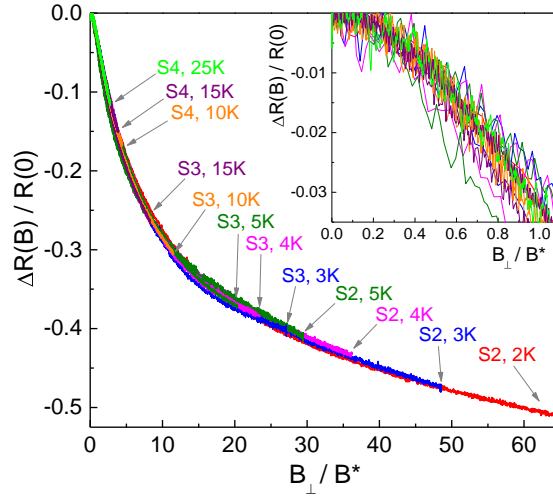


Fig. 7. The NMR data for different samples and different temperatures plotted as a function of dimensionless magnetic field  $B_{\perp}/B^*$ . The arrows and numbers show the end of each curve and indicate the sample (2, 3, 4) and  $T$ . In insert, the NMR data are shown for small values  $B_{\perp}/B^* < 1$ .

### Positive MR in parallel magnetic fields

In parallel magnetic fields, PMR is observed at low temperatures, Fig. 1. Very small NMR at high temperatures could be explained as the traces of NMR due to the possible folds on the surface of monolayer graphene film, where the parallel magnetic field has a

perpendicular influence component. PMR appears only at low temperatures, at  $T < 5$  K and increases with decreasing  $T$ . PMR is proportional to  $B_{\parallel}^2$  at low fields, and becomes linear with increasing  $B$  (Fig. 8).

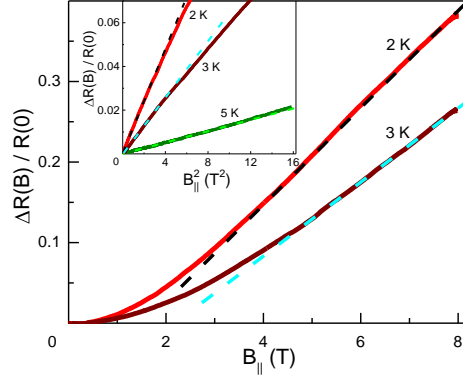


Fig. 8. PMR of sample 3 plotted as a function of  $B_{\parallel}$ . In insert, PMR data for low fields are plotted on a quadratic scale.

PMR in parallel magnetic fields has been observed in 2d VRH regime in different systems: in  $\text{Al}_x\text{In}_{1-x}\text{Sb}/\text{InSb}$  quantum well [15], in single layer of  $\text{GaAs}/\text{Al}_x\text{Ga}_{1-x}\text{As}$  heterostructure [27]. Because the parallel magnetic field couples only to the electron spin, it means that the spin state of localized electrons influences the hopping conductivity despite the fact that it is not included explicitly in the expressions for VRH, Eqs. (1) and (2). The explanatory models of this effect are based on two ideas. The authors [28] considered the case when an intermediate scatterer (see Fig. 4) should be occupied to produce a negative scattering amplitude. Thus, the interference is depended on the mutual spin orientation of hopping electron and electron localized on scattering center. In magnetic fields, all localized spins are aligned which increases the destructive interference and results in increase of the resistance. Another mechanism was suggested by Kurobe and Kamimura [29] and studied in [30]. In this model, it is recognized that a certain fraction of the states can accommodate two electrons. Double occupancy is possible if the on-site Coulomb repulsion  $U$  between the electrons is smaller than the width of the energy distribution function of the localized states. It was already mentioned that in VRH, only localized states with energy level within the narrow optimal band of width  $\varepsilon(T)$  around  $\mu$  are involved in the hopping process, Eq. (3). However, for some states, which cannot participate in VRH at given temperature because the energy of the first electron  $\varepsilon^{(1)}$  is well below  $\mu$ , the energy of the second electron  $\varepsilon^{(2)} = \varepsilon^{(1)} + U$  may be located just within the optimal band, Fig. 9. This allows those states to participate in the VRH at zero magnetic field. In strong field limit, all spins are polarized and, therefore, transitions through the double occupied states are suppressed which results in increase of resistance.

Fig. 1 shows that PMR is observed in our samples only at low temperatures. We think that this fact supports the mechanism [29] based on participation of the double occupied states, because the first mechanism [28] has no limitation for observation at all temperatures. In the second mechanism, however, contribution of the double occupied states in VRH is important only when the width of the optimal band  $\varepsilon(T)$  which decreases

with decreasing  $T$ , becomes less than  $U$ , otherwise in the case of opposite inequality,  $U \ll \varepsilon(T)$ , the localized states will either participate or not participate in VRH independently of the existence of the double occupied states. At weak magnetic fields, theory [30] predicts the linear dependence  $\Delta R/R \sim (g_L \mu_B B)/T$ , where  $g_L$  is the Lande-factor and  $\mu_B$  is the Bohr magneton, while at weak fields one expect the quadratic dependence  $\Delta R/R \sim B^2$ . This agrees with experiment (Fig. 8). Theory predicts also saturation PMR at strong fields when all electron spins are polarized. In our samples, no tendency to saturation was observed in magnetic fields up to 8 T.

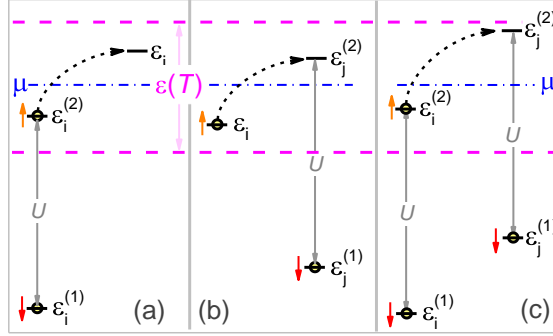


Fig. 9. Schematic representation of the possible hopping transition via the double occupied states where the double occupied is an initial  $\varepsilon_i$ (a), final  $\varepsilon_j$ (b) or both initial and final states (c).  $\mu$  represents the position of the Fermi level, dashed lines show the width  $\varepsilon(T)$  of the optimal band at given temperature, Eq. (3).

In conclusion, MR of strongly disordered monolayer graphene films with VRH mechanism of conductivity was measured in perpendicular  $B_\perp$  and parallel  $B_\parallel$  magnetic fields. It is shown that in  $B_\perp$ , resistance decreases (negative MR), while  $B_\parallel$  leads to the positive MR at low temperatures. The NMR effect is explained in the framework of the “orbital” mechanism based on the interference of many paths through the intermediate sites in the probability of the long-distant tunneling in the VRH regime. Magnetic field  $B^*$  at which the quadratic dependence  $\Delta R/R \sim B^2$  is replaced by the linear one is determined as the merging parameter. It was shown that  $B^* \sim T^{1/2}$  in accordance with theory. The localization radius  $\xi$  for samples with different dose of irradiation was calculated. It is found that, expectedly,  $\xi$  decreases with increase of disorder. It is shown also that all NMR curves for different samples and different temperatures are merged in one common curve when plotted on normalized scale  $B/B^*$ . The PMR effect is observed at low  $T$  and could be explained by suppression in a strong magnetic field the hopping transitions via double occupied states due to electron spin polarization.

†e-mail: [ishlimak@gmail.com](mailto:ishlimak@gmail.com)

‡permanent address: Soreq NRC, Yavne 8180000, Israel

## References

- [1] D. C. Elias, R. R. Nair, T. M. G. Mohiuddin, S. V. Morozov, P. Blake, M. P. Halsall, A. C. Ferrari, D. W. Boukhvalov, M. I. Katsnelson, A. K. Geim, K. S. Novoselov, *Science* **323**, 610 (2009).
- [2] J.P. Robinson, H. Schomerus, L. Oroz lany, and V. Fal'ko, *Phys. Rev. Lett.* **101**, 196803 (2008).
- [3] Jian-Hao Chen, W.G. Cullen, C. Jang, M.S. Fuhrer, and E.D. Williams, *Phys. Rev. Lett.* **102**, 236805 (2009).
- [4] X. Hong, S.-H. Cheng, C. Herding, and J. Zhu, *Phys. Rev. B* **83**, 085410 (2011).
- [5] J. Moser, H. Tao, S. Roche, F. Alzina, C.M. Sotomayor Torres, and A. Bachtold, *Phys. Rev. B* **81**, 205445 (2010).
- [6] Shu-Wei Wang, H.E Lin, Huang-De Lin, K.Y Chen, Kun-Hua Tu, C.W Chen, Ju-Ying Chen, Cheng-Hua Liu, C-T Liang and Y.F Chen, *Nanotechnology* **22**, 335701 (2011).
- [7] Yang-Bo Zhou, Bing-Hong Han, Zhi-Min Liao, Han-Chun Wu and Da-Peng Yu, *Appl. Phys. Lett.* **98**, 222502 (2011).
- [8] Jian-Hao Chen, W. G. Cullen, C. Jang, M. S. Fuhrer, and E. D. Williams, *Phys. Rev. Lett.* **102**, 236805(2009).
- [9] G. Buchovicz, P.R. Stone, J.T. Robinson, C.D. Gress, J.W. Beeman, and O.D. Dubon, *Appl. Phys. Lett.* **98**, 032102 (2011).
- [10] I. Shlimak, A. Haran, E. Zion, T. Havdala, Yu. Kaganovskii, A.V. Butenko, L. Wolfson, V. Richter, D. Naveh, A. Sharoni, E. Kogan and M. Kaveh, *Phys. Rev. B* **91**, 045414 (2015).
- [11] E. Zion, A. Haran, A.V. Butenko, L. Wolfson, Yu. Kaganovskii, T. Havdala, A. Sharoni, D. Naveh, V. Richter, M. Kaveh, E. Kogan and I. Shlimak, arXiv:1501.04581, submitted to PRB.
- [12] E. McCann, K. Kechedzhi, Vladimir I. Fal'ko, H. Suzuura, T. Ando, and B. L. Altshuler, *Phys. Rev. Lett.* **97**, 146805 (2006).
- [13] B.I. Shklovskii and A.L. Efros, *Electronic Properties of Doped Semiconductors* (Springer-Verlag, Berlin, 1984).
- [14] I. Shlimak, *Is Hopping a Science? Selected Topics of Hopping Conductivity* (World Scientific, Singapore, 2015), Chapter 4.
- [15] S. Ishida, T. Manago, K. Oto, A. Fujimoto, H. Geka, A. Okamoto, and I. Shibusaki, in: *Narrow Gap Semiconductors 2007*, Ed. by B. Murdin and S.K. Clowes. (Springer Proceedings in Physics) **119**, 203 (2008).
- [16] E.I. Laiko, A.O. Orlov, A.K. Savchenko, E.A. Il'ichev, and E.A. Poltoratskii, *Sov. Phys. JETP* **66**, 1258 (1987).
- [17] F.P. Milliken and Z. Ovadyahu, *Phys. Rev. Lett.* **65**, 911 (1990).

- [18] Qiu-yi Ye, B. I. Shklovskii, A. Zrenner, F. Koch, and K. Ploog, *Phys. Rev. B* **41**, 8477 (1990).
- [19] H.W. Jiang, C.E. Johnson, and K.L. Wang, *Phys. Rev. B* **46**, 12830 (1992).
- [20] V.F. Mitin, V.K. Dugaev, and G.G. Ihas, *Appl. Phys. Lett.* **91**, 202107 (2007).
- [21] V.L. Nguen, B.Z. Spivak and B.I. Shklovskii, *JETP Lett.* **41**, 42 (1985); *Sov. Phys. JETP*, **62**, 1021 (1985).
- [22] O. Entin-Wholman, Y. Imry and U. Sivan, *Phys. Rev. B* **40**, 8342 (1989).
- [23] B.I. Shklovskii and B.Z. Spivak, in: *Hopping Transport in Solids*, Ed. by M. Pollak and B. Shklovskii (Elsevier, Amsterdam, The Netherlands, 1991), p. 217.
- [24] M.E. Raikh, G.F. Wessels, *Phys. Rev. B* **47**, 15609 (1993).
- [25] W. Schirmacher, *Phys. Rev. B* **41**, 2461 (1990).
- [26] L.B. Ioffe, B.Z. Spivak, *Sov. Phys. JETP*, **144**, 632 (2013).
- [27] I. Shlimak, S. I. Khondaker, M. Pepper, D.A. Ritchie, *Phys. Rev. B* **61**, 7253 (2000).
- [28] H.L. Zhao, B.Z. Spivak, M.P. Gelfand, and S. Feng, *Phys. Rev. B* **44**, 10760 (1991).
- [29] A. Kurobe and H. Kamimura, *J. Phys. Soc. Japan* **51**, 1904 (1982).
- [30] K.A. Matveev, L.I. Glazman, P. Clark, D. Ephron, M.R. Beasley, *Phys. Rev. B* **52**, 5289 (1995).